

# LIQUIDS POTENTIAL OF THE LOWER TO MIDDLE TRIASSIC MONTNEY AND DOIG FORMATIONS, BRITISH COLUMBIA

Filippo Ferri<sup>1</sup>, Mark Hayes<sup>2</sup> and Aaron Nelson<sup>3</sup>

## ABSTRACT

Zones of dry gas, wet gas and oil potential within the Montney Formation were outlined using  $T_{max}$  values from Rock Eval™ analysis of core and cuttings, and from raw gas production and allocated gas plant sales data.

Results from both techniques are, for the most part, in general agreement, but discrepancies are present in the southern part of the Montney play trend. These departures may be either due to the suppression of the  $T_{max}$  value by migrated oil/bitumen or contamination by oil-based drilling fluids. Alternatively, low production of liquids in the southern Montney trend may be the result of a higher percentage of type III kerogen, which produces considerably less liquid hydrocarbons.

Ferri, F., Hayes, M. and Nelson, A. (2013): Liquids potential of the Lower to Middle Triassic Montney and Doig formations, British Columbia; in Geoscience Reports 2013, *British Columbia Ministry of Natural Gas Development*, pages 1–11.

<sup>1</sup>Geoscience and Strategic Initiatives Branch, Oil and Gas Division, British Columbia Ministry of Natural Gas Development, Victoria, British Columbia, Fil.Ferri@gov.bc.ca

<sup>2</sup>Operations Division, Resource Development and Geology, British Columbia Oil and Gas Commission, Victoria, British Columbia

<sup>3</sup>Royalty Policy Branch, Oil and Gas Division, British Columbia Ministry of Natural Gas Development, Victoria, British Columbia

**Key Words:** Montney, Doig, natural gas liquids, condensate, oil, Rock Eval, thermal maturity, natural gas processing, production, plant sales

## INTRODUCTION

The production of natural gas in British Columbia is now primarily from tight and shale gas reservoirs, the bulk originating from the Montney Formation (Figs. 1, 2). The current rate of development within the Montney Formation is not only an indication of the more favourable reservoir characteristics (porosity, organic carbon content, pressures), but also a reflection of the higher natural gas liquid (C2–C4) and condensate (C5–C12) concentrations of the formation, the latter of which adds considerable value to well production during this period of low natural gas prices.

Considering the increased level of Montney liquids<sup>1</sup> production in the province (Fig. 3), understanding the spatial distribution (i.e., mapping) of this potential will be critical. This is true not only from an economic standpoint, but also from a developmental and royalty perspective. The mapping of the liquids potential within the Montney Formation was attempted through compilation and contouring of 1) thermal maturity data (Rock Eval, reflectance microscopy) found within published reports, papers and well data

submission and 2) liquids production per unit volume of gas produced.

An outcome of this exercise has been a more readily available dataset of well-head liquids production. The well-head production of liquids is calculated at the gas plant based on well-head gross gas production and gas analysis. Historically, this information has been kept by the British Columbia Ministry of Finance, but it has now been supplied to the British Columbia Oil and Gas Commission and procedures are being implemented to publically distribute this dataset.

## THERMAL MATURITY

Thermal maturity data for the Montney and Doig formations were obtained from several sources, including 1) regional Rock Eval analysis of cuttings across northeastern British Columbia and Alberta carried out by the Geological Survey of Canada (Riediger, 1990; Snowdon, 2000; Fowler and Snowdon, 2001, 2007a, b); 2) compilation of core and cutting analysis produced by the British Columbia Ministry

<sup>1</sup>In this paper, the term 'liquids' is used in reference to natural gas liquids (C2–C4) and condensate (C5 and higher) production.

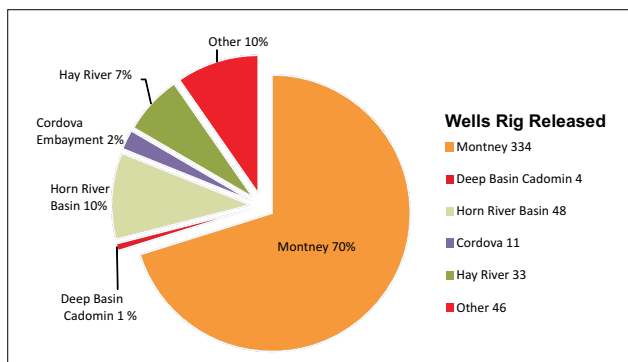


Figure 1. The percentages of production from formations in north-eastern British Columbia in 2012. Also shown are the number of wells drilled during 2012, based on rig release data.

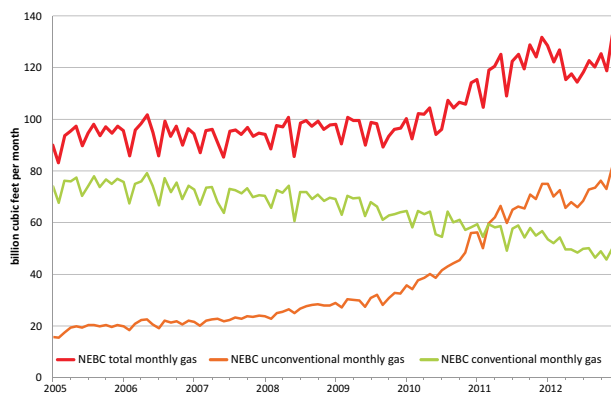


Figure 2. Overall production from conventional and unconventional reservoirs, north-eastern British Columbia (NEBC: north-eastern British Columbia).

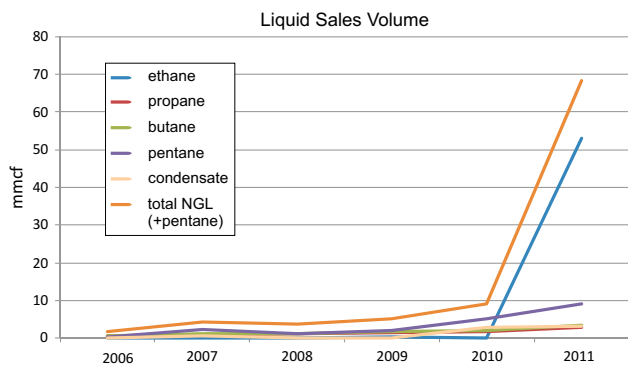


Figure 3. Liquids (natural gas liquids [NGL] and condensate) sales volume in British Columbia from 2006 to 2011, in million cubic feet (mmcf).

of Energy, Mines and Natural Gas (Walsh et al., 2007; Ferri et al., 2013); and 3) published papers (Ibrahimbas and Riediger, 2004).

The majority of thermal maturity data used in this report was part of Rock Eval/total organic carbon (TOC) datasets. In Rock Eval analysis, the  $T_{\max}$  value is used as a measure of the thermal maturity of the kerogen within an organic-rich sample. During Rock Eval pyrolysis,  $T_{\max}$  is

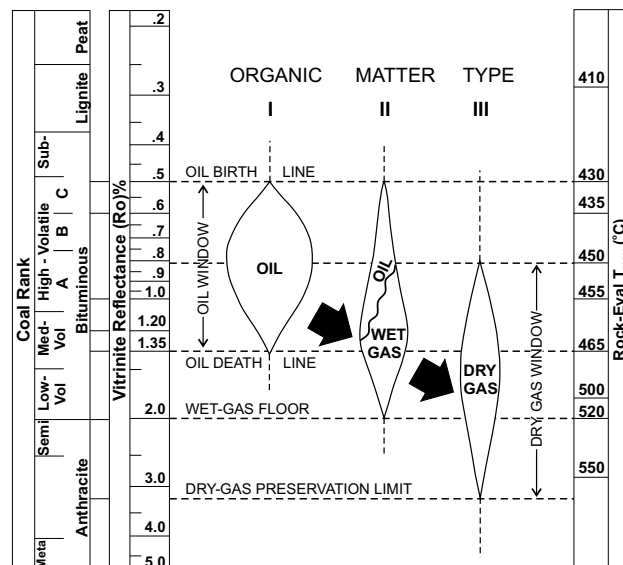


Figure 4. Zones of petroleum generation and destruction.

the temperature recorded at the S2 peak; i.e., the temperature at the maximum production of hydrocarbons during stepwise heating of a sample (Fig. 5). Experimental data has shown that this temperature increases in conjunction with the maximum paleotemperatures recorded by the rock (Peters, 1986; Fig. 4). This temperature is also sensitive to the type of kerogen present in the rock (Fig. 5). Empirical data has shown a direct correlation between specific  $T_{\max}$  values and the production and preservation of petroleum in the rock column (Fig. 4; Peters, 1986).

Reflectance microscopy of organic matter, primarily of coal macerals (i.e., vitrinite) is the most common and robust method for determining the level of thermal maturation in an organic-rich sedimentary rock (Dow, 1977). There is a positive linear relationship between the amount of light reflected from a polished maceral immersed in oil (%Ro) and the degree of thermal maturation the maceral has attained, i.e., the amount of reflected light increases with maturation. In the long history of coal exploration, thermal maturity based on reflectance data from vitrinite has become the reference parameter for stating the thermal maturity of a rock and reflectance data from other organic macerals are converted to the vitrinite values following a linear correlation (Jacob, 1985). Furthermore, there is a correlation between vitrinite reflectance and  $T_{\max}$  values that is shown graphically in Figure 4 (Teichmuller and Durand, 1983; Lafargue et al., 1998). Reflectance microscopy thermal maturity data from well file reports were converted to  $T_{\max}$  values based on the relationships shown by Lafargue et al. (1998) and Teichmuller and Durand (1983).

Thermal maturity values for 88 wells were compiled using  $T_{\max}$  and reflectance microscopy values (Table 1). Due to the dominance of  $T_{\max}$  data, vitrinite or equivalent data were converted to  $T_{\max}$  based on several correlations

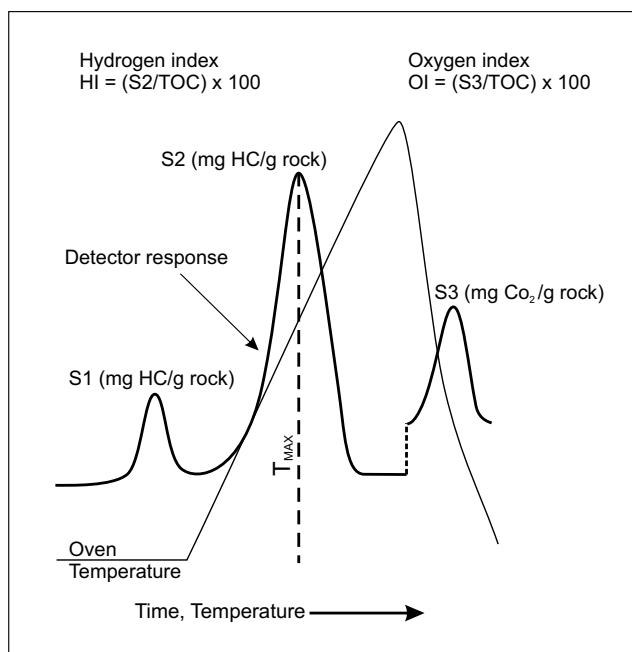


Figure 5. Schematic representation of the Rock Eval program. This instrument uses a ramped temperature pyrolysis process whereby a small amount of sample (70–100 mg) is heated in an inert atmosphere (helium or nitrogen). Any volatile hydrocarbons (i.e., those adhered to organic carbon or in pore spaces) will be released when the sample is initially heated to 300°C and the amount is referenced as the S1 peak. The sample is then heated to 600°C at 25°C/min and hydrocarbons generated during this ramped heating are produced from the cracking of kerogen in the sample. The amount of hydrocarbons produced is called S2.  $T_{max}$  is the temperature of maximum hydrocarbon generation during this stepped heating. A separate detector registers the amount of CO and CO<sub>2</sub> generated, which gives the S3 value. The sample is then exposed to oxygen so that any remaining organic carbon is combusted and measured. Together with data from S1, S2 and S3, it is used to calculate the total organic carbon (TOC). A pyrogram showing the response of the detectors through time (and heating) is also produced and can provide additional information.

S1 and S2 are reported in milligrams of hydrocarbons generated from kerogen in 1 g of rock (mg HC/g rock). S3 represents milligrams of CO<sub>2</sub> generated from 1 g of rock. The hydrogen index (HI) is calculated from S2 and corresponds to the quantity of pyrolyzable organic matter (i.e., hydrocarbons, HC) that can be generated from 1 g of organic carbon (mg HC/g TOC). The oxygen index (OI) is calculated from S3 and represents the amount of CO<sub>2</sub> in 1 g of organic carbon (mg CO<sub>2</sub>/g TOC).

and then averaged (Lafargue et al., 1998; Dewing and Sanei, 2009). Rock Eval data was first filtered using TOC and S2 cutoffs of 0.3 wt.% and 0.2 mg HC/g rock, respectively. Practice has shown that Rock Eval parameters have little significance when TOC levels are below this value and  $T_{max}$  results are suspect when S2 is lower than 0.2 mg HC/g rock (Espitalié et al., 1985a, b, 1986; Peters, 1986).

Proper filtering of  $T_{max}$  data is difficult in the absence of pyrograms. Some of the datasets show anomalously low

$T_{max}$  values (Snowdon, 2000), even within acceptable TOC and S2 parameters, suggesting either migrated oil into the sample or the use of oil-based mud additives (Peters, 1986). A systematic search of the well files to determine the mud composition during drilling of the Montney-Doig succession was not performed. In other instances, initial contour maps generated from averaged  $T_{max}$  values produced noticeable anomalies or ‘bull’s eyes’ on the map. This led to the re-inspection of datasets and filtering based on modified criteria such as higher S2 cutoffs.

Although the Montney-Doig succession can be several hundreds of metres thick in the western part of the basin (Fig. 6), the scatter and distribution of  $T_{max}$  values in wells with relatively complete datasets does not indicate an overall increase with depth (Fig. 7). As such,  $T_{max}$  values for wells where data was available was averaged (88 data points, Table 1), spatially positioned and contoured (Fig. 8). Rock Eval analysis of Montney and Doig rocks indicates a predominance of type II/III kerogen (Figs. 4, 9). Unbiased contouring shows an overall maturity increase outlining the Deep Basin (as would be expected), with the peak wet gas line ( $T_{max} = 460^{\circ}\text{C}$  to  $465^{\circ}\text{C}$ ; Fig. 4) trending diagonally, northwestward through the Peace River block and then northward (Fig. 8). Wells east of this line should have production that is richer in liquids and wells east of the  $450^{\circ}\text{C}$   $T_{max}$  value should have production dominated by oil.

## LIQUIDS PRODUCTION

Although thermal maturation data can predict regions of oil, gas or wet gas potential within a formation, production records, if available in enough detail and numbers, can be spatially plotted to predict similar prospectivity. Current well counts within the Montney Formation, together with production statistics, are large enough to allow this exercise to be performed with a degree of confidence (Figs. 10–12).

Although the British Columbia Oil and Gas Commission captures the production of raw gas and some condensate at the well head, due to the centralized nature of natural gas processing, an accurate tabulation of condensate and natural gas liquids production can only be accomplished through the compilation of processing plant sales data, which are housed with the British Columbia Ministry of Finance (Fig. 13). Although condensate can be removed in the field (Fig. 13c), it is more economic to keep it in the gas stream and process it at a centralized facility. Separation of condensate in the field is dependent on the amount and composition of the condensate (e.g., amount of waxes) and distance to the nearest gas plant. When the condensate concentration exceeds approximately 50 barrels per million cubic feet of raw gas (0.28 m<sup>3</sup>/e<sup>3</sup>m<sup>3</sup>), it is necessary to separate the condensate from the raw gas stream and measure the two streams separately to accurately calculate the amount of each component before sending the combined

TABLE 1. LIST OF WELLS USED IN THE STUDY AND AVERAGE T<sub>max</sub> VALUES FOR ANALYZED CORE AND/OR CUTTINGS FROM THE MONTNEY AND DOIG FORMATIONS.

UWI	WA	T <sub>max</sub>	n	UWI	WA	T <sub>max</sub>	n
11-4-79-14W6	17427	451 ±3	5	6-10-85-25W6	5704	465 ±2	2
9-31-79-14W6	13426	451 <sup>+</sup>	2	8-11-87-25W6	182	457 ±4	14
13-1-77-15W6	10621	445	1	b-4-L/93-P-7	5465	472	1
7-13-79-15W6	16639	463 ±9 <sup>+</sup>	10	a-20-H/93-P-9	16615	475 <sup>+</sup>	2
11-31-79-15W6	6877	462 ±4	5	d-39-F/93-P-9	10562	470 ±4 <sup>+</sup>	2
1-36-79-15W6	16425	450 ±2 <sup>+</sup>	4	b-32-G/93-P-9	10766	452 ±7 <sup>*</sup>	15
10-22-80-15W6	7149	453 ±6 <sup>*</sup>	11	b-32-G/93-P-9	13006	451 ±4	1
15-8-78-16W6	10690	452	1	a-29-H/93-P-9	10385	443 ±8	2
16-15-78-16W6	14756	438	1	a-38-H/93-P-9	16536	471 ±14 <sup>+</sup>	10
8-10-79-16W6	10761	463 ±3	3	b-64-I/94-A-12	4914	447 ±1	2
11-18-79-16W6	5007	476	1	c-21-L/94-A-13	24759	464 ±15	18
12-25-79-16W6	5364	463 ±8	7	d-69-J/94-A-15	2832	447 ±3	32
11-35-79-16W6	7485	454 ±7	7	a-59-G/94-A-16	1832	442 ±2	8
1-26-86-16W6	208	441 ±3	30	c-74-I/94-B-1	24302	473 ±13 <sup>*</sup>	9
13-33-78-17W6	24564	456 ±10	32	a-39-E/94-B-8	951	480 ±4	38
14-35-78-17W6	10677	447 ±16	2	c-44-L/94-B-8	25155	491 ±13	9
15-26-79-17W6	24170	461 ±5 <sup>*</sup>	16	a-10-J/94-B-9	25161	483 ±20	12
14-34-79-17W6	23576	446 ±3	3	c-33-C/94-B-9	25738	453 ±12	33
8-8-80-17W6	23233	454 ±10	4	d-67-J/94-B-9	25311	490 ±10	6
11-11-80-17W6	2378	452 ±6	5	c-74-B/94-B-9	4205	449 ±8	5
4-27-88-17W6	130	453 ±3	4	d-87-I/94-B-14	554	504 ±12	15
9-33-78-18W6	24241	441 ±2 <sup>*</sup>	8	a-86-C/94-B-15	827	478 ±16	7
15-34-80-18W6	24410	454 ±9	57	d-8-F/94-B-16	26622	472 ±8	9
8-10-84-18W6	6294	463	2	d-50-H/94-B-16	25568	467 ±11	21
11-28-78-19W6	25466	457 ±12	25	d-38-J/94-B-16	18509	456 ±4 <sup>*</sup>	10
8-8-81-19W6	24288	451 ±6	31	b-69-A/94-B-16	253	452 ±10	30
6-17-86-19W6	1770	446 ±5	14	d-100-J/94-B-16	25392	458 ±9	4
13-21-77-20W6	24268	464	1	a-78-C/94-G-1	25788	465 ±7	16
16-29-79-20W6	25478	461 ±16	43	c-54-B/94-G-7	25640	477 ±11	22
13-11-81-20W6	24354	457 ±9	19	c-80-L/94-G-7	647	472 ±8	2
8-22-82-20W6	21910	459 ±9	11	b-10-C/94-H-1	2052	451 ±2	2
3-30-82-20W6	23346	445 ±3	5	d-13-D/94-H-1	5586	447	2
14-16-83-20W6	26789	458 ±5	14	d-25-D/94-H-1	2278	451 ±1	2
16-8-86-20W6	6124	446 ±6	7	d-81-E/94-H-1	2916	455 ±1	2
11-10-86-20W6	1190	439 ±4	34	a-78-F/94-H-1	920	443 ±4	4
8-14-86-20W6	6734	449 ±2	2	d-48-H/94-H-1	1433	436 ±4	2
7-5-87-20W6	2338	458 ±4	10	d-49-J/94-H-1	5294	434 ±2	15
4-11-81-21W6	25261	465 ±15	66	d-4-B/94-H-2	1748	451 ±2	2
3-1-83-21W6	26335	459 ±4	18	b-92-G/94-J-2	15973	464 ±9	7
11-19-83-21W6	4598	461 ±3	4	c-86-D/94-J-12	2150	455	1
10-24-86-21W6	2243	461 ±6	4	d-72-E/94-H-2	2044	444 ±3	11
13-8-82-22W6	26283	471 ±7	5	a-79-B/94-H-4	61	459 ±11	21
1-12-84-23W6	108	450 ±2	10	d-45-G/94-H-9	10189	435 ±3	4
16-17-83-25W6	25450	481 ±10	4	b-16-H/94-H-13	916	442 ±5	12

\*Includes R<sub>o</sub> values

UWI: Universal well Identifier  
n: number of measurements

<sup>+</sup>R<sub>o</sub> values only

WA: Well Authorization

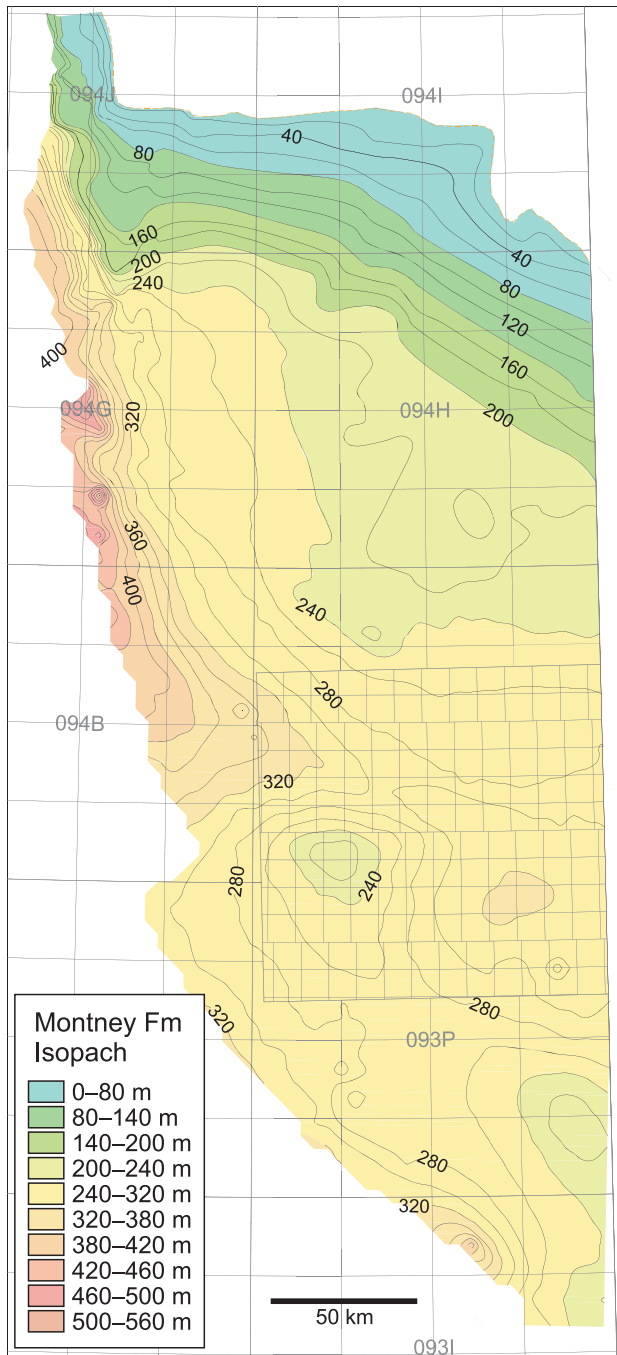


Figure 6. Isopach map of the Triassic Montney and Doig formations.

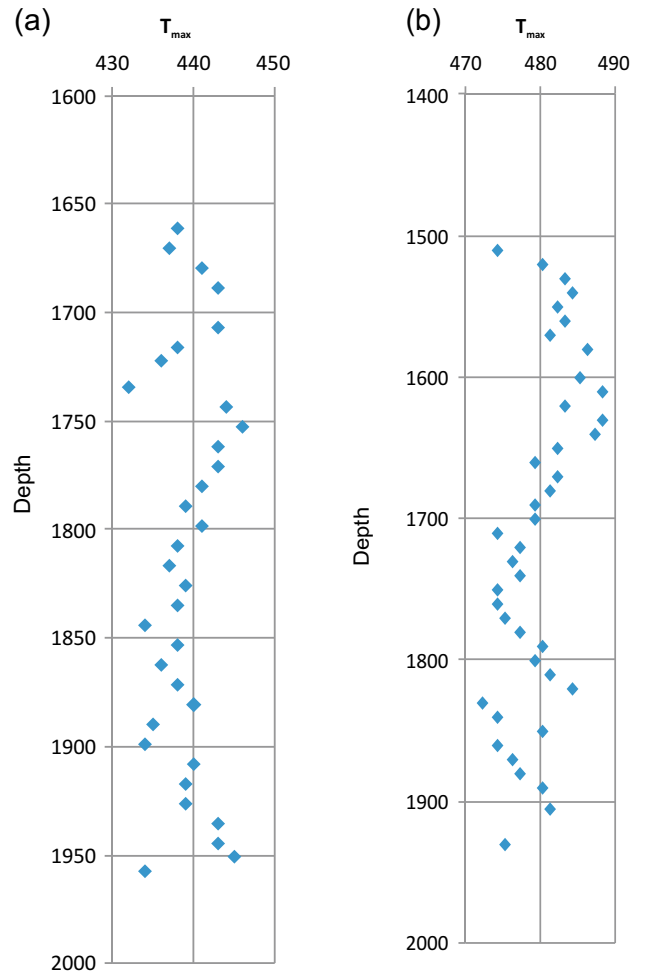


Figure 7.  $T_{max}$  versus depth for samples from the Montney and Doig formations: a) 11-10-86-20W6; b) c-029-E/94-B-08. Note that the scatter of data does not show an increase with depth.

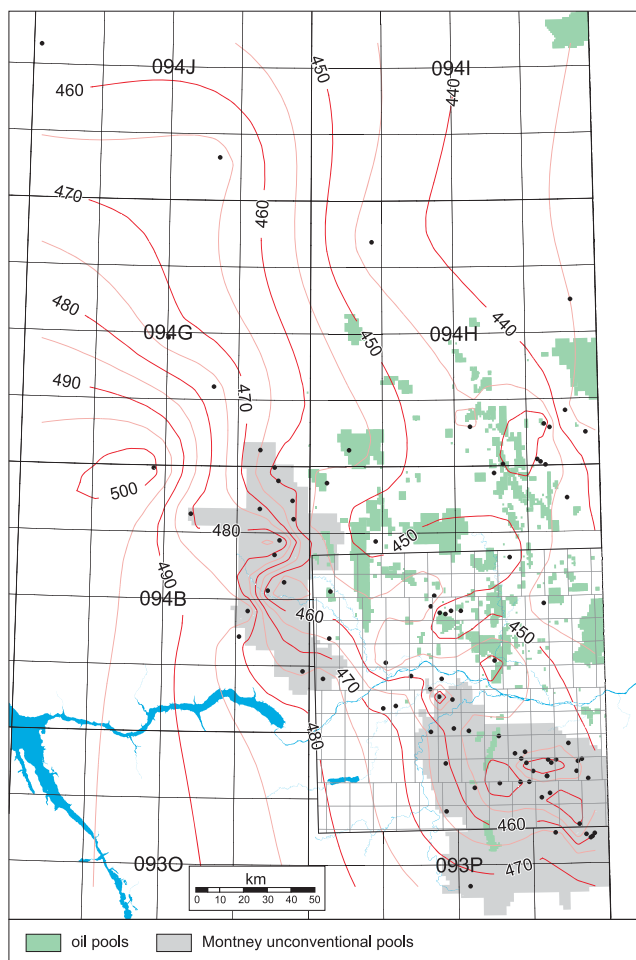
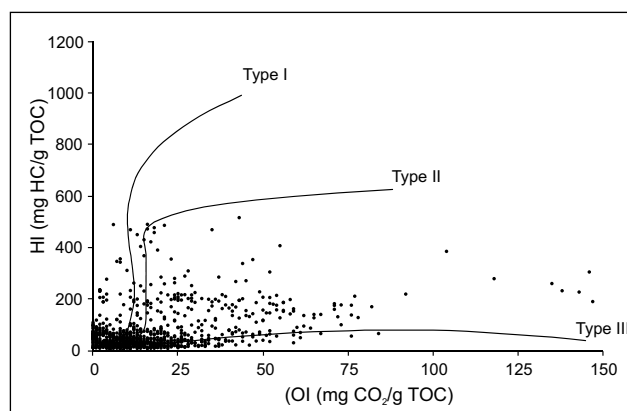


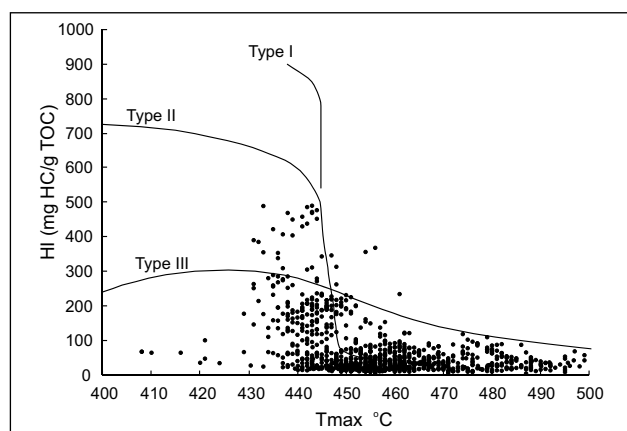
Figure 8. Contoured  $T_{max}$  values, Montney-Doig formations. This was performed using Surfer 8™ software within GeoSCOUT™, using a kriging gridding method.

stream to the gas plant (Fig. 13b). The quantity of condensate is converted to a raw gas stream equivalent. Assigning production from a natural gas processing facility back to individual wells is calculated from a compositional analysis and flow rate of the raw gas stream.

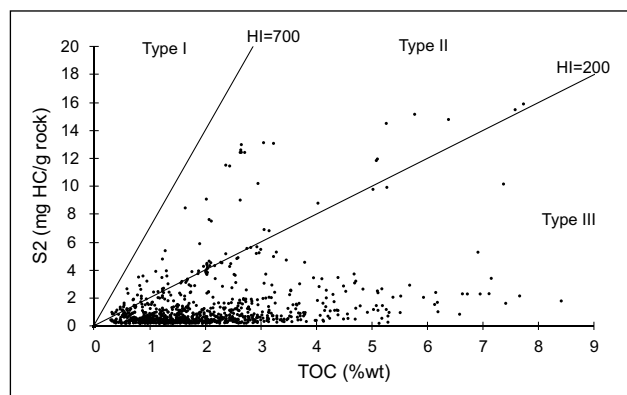
Natural gas processing plants have different capabilities and efficiencies; i.e., some only separate condensate, whereas others also have a natural gas liquids stream. Because facilities with the capacity to remove ethane (i.e., ‘deep cut’ plants) are not common, ethane-bearing gas is sold at a higher premium due to the increased caloric value. This gas can be sold directly to the end user or may be removed by more efficient gas plants in a downstream location (Fig. 13).



a)



b)



c)

Figure 9. a) Modified van Krevelen diagram (Tissot and Welde, 1984) based on filtered Rock Eval analysis of Montney and Doig samples from wells listed in Table 1; b) HI versus  $T_{max}$  diagram based on filtered Rock Eval analysis of Montney and Doig samples from wells listed in Table 1 (modified from Bordenave, 1993); c) S2 versus total organic carbon (TOC) diagram based on filtered Rock Eval analysis of Montney and Doig samples from wells listed in Table 1 (modified from Langford and Blanc-Valleron, 1990).

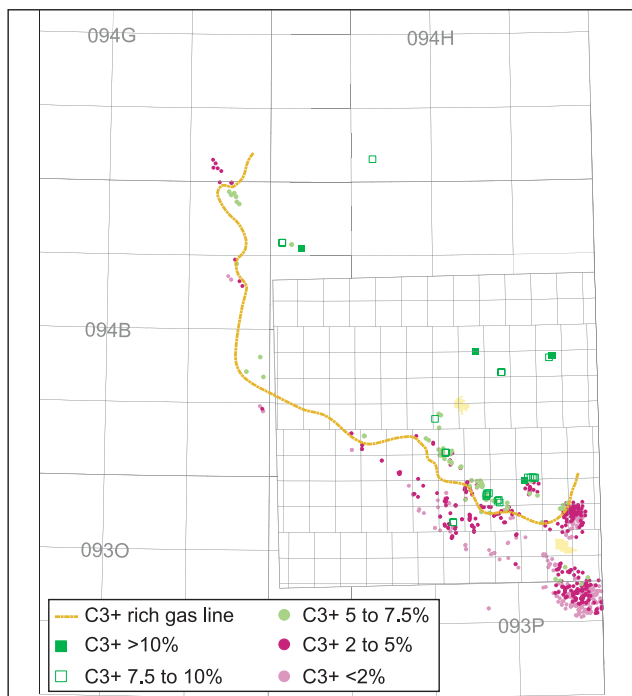


Figure 10. Gas analysis for Montney Formation production showing C3 and greater concentrations.

## DISCUSSION

An attempt at outlining zones of predominantly dry gas, wet gas, wet gas to oil and oil, based on mapping of  $T_{max}$  values and sales gas data is shown in Figures 14 and 15. Trends in the northern parts of both maps generally define the same zones. Although detailed sales data for the Heritage and Northern Montney fields has allowed differentiation into dry gas, wet gas and oil zones, lack of data between the two areas does not permit the same level of differentiation. It is likely that the wet gas zone and the oil zone extend to the northwest, as predicted by the thermal maturation data.

Oil to gas zones, as defined by the two methods, do not define the same trends along the southern part of the Peace River block and into the 094P map area (Figs. 14, 15). Pockets of higher liquids production are found in the dry gas zone of the southern Peace River block shown in Figure 15 (see C3 and greater gas analysis trends, C3+C4 production and pentane [C5] plus production, Figs. 10–12) and may support the lower thermal maturities defined by  $T_{max}$  values.

Gas and liquids data is very robust in the southern Peace River block, suggesting issues with the Rock Eval data. Rock Eval data cluster in this part of the study area (Figs. 8, 14, Table 1), which display a considerable range of  $T_{max}$  values (438–476°C), although the majority fall between 440–455°C. As discussed previously, suppression of  $T_{max}$  values can occur due to sample contamination from oil-based drilling fluids or from migrated oil or bitumen in

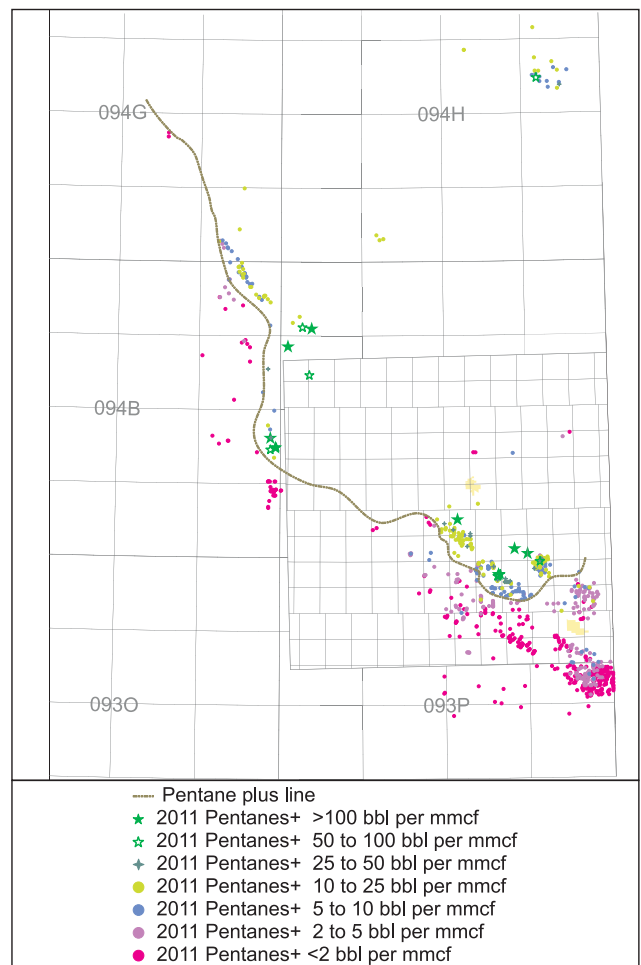


Figure 11. Liquids production map for the Montney Formation showing C5 and greater production in barrels per million cubic feet of gas.

the sample (Peters, 1986). As the original pyrograms are not available, testing either of these hypotheses would require determination of drilling fluids from drilling records and/or petrographic analysis of cuttings and core.

An alternative explanation for the lower liquids content of the wells in this area may be related to the type of kerogen present within Montney rocks. Type II/III kerogen is suggested by the Rock Eval dataset (Fig. 9) and has been described by other workers (Riediger, 1990). If kerogen in this area is closer to type III in nature, then its ability to produce liquid hydrocarbons would be considerably less than type II kerogen (Jarvie, 1991).

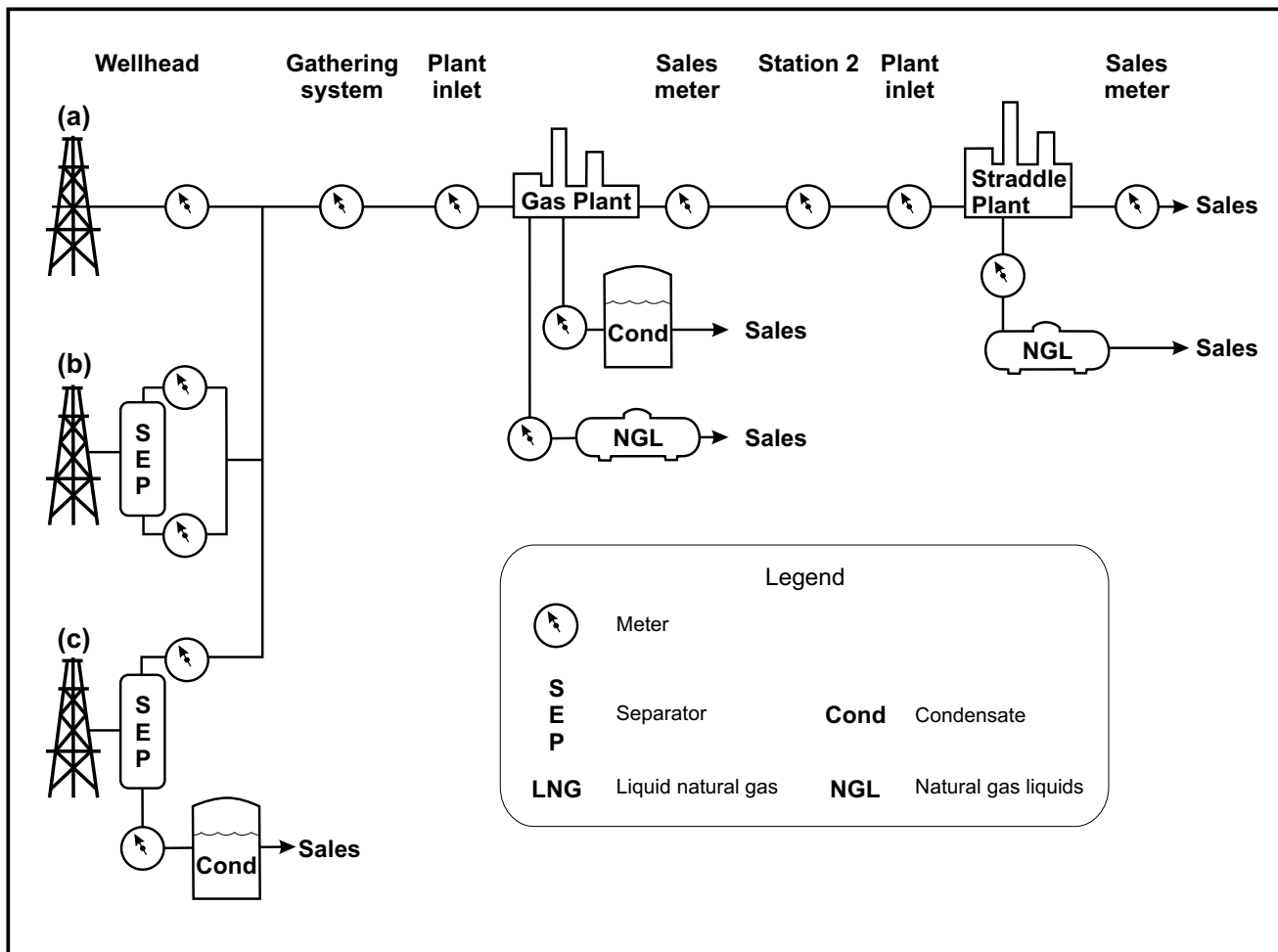


Figure 13. Three scenarios for production and processing of raw gas streams with varying proportions of condensate and natural gas liquids. In all scenarios, allocation of natural gas plant production back to the individual wells is based on both the compositional analysis and absolute flow rate of raw gas. The type of natural gas liquids produced depends on the capabilities of the gas plant; i.e., 'deep cut' plants can effectively remove ethane (C<sub>2</sub>) from the gas stream: a) Raw gas production contains less than 50 barrels of condensate per million cubic feet of gas (0.28 m<sup>3</sup>/e3m<sup>3</sup>) and is sent directly to the processing plant; b) Raw gas production contains greater than 50 barrels of condensate per million cubic feet of gas (0.28 m<sup>3</sup>/e3m<sup>3</sup>). An accurate determination of raw gas production requires separation and measurement of condensate, and conversion of condensate composition to an equivalent raw gas stream flow rate; c) Condensate is removed at the well head and shipped to a sale point. Remaining liquids-rich gas is sent to the gas plant for processing.

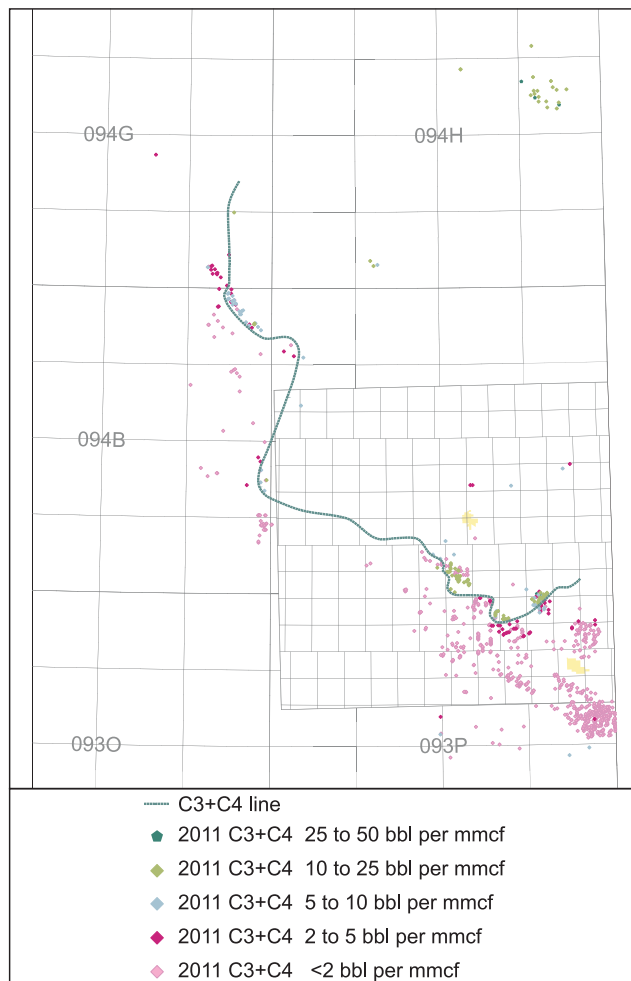


Figure 12. Liquids production for the Montney Formation showing C3+C4 production in barrels per million cubic feet of gas.

## CONCLUSIONS

- Gas and liquids potential trends within the Montney Formation were determined using both  $T_{max}$  values from Rock Eval analysis of core and cuttings, and from raw gas production and gas plant sales data.
- Results from both techniques are for the most part in general agreement, but discrepancies are present in the southern part of the Montney play trend.
- These deviations may either be due to the suppression of the  $T_{max}$  value by migrated oil/bitumen or contamination by oil-based drilling fluids. Alternatively, the low production of liquids in the southern Montney trend may be due to a higher percentage of type III kerogen, which produces considerably less liquid hydrocarbons.

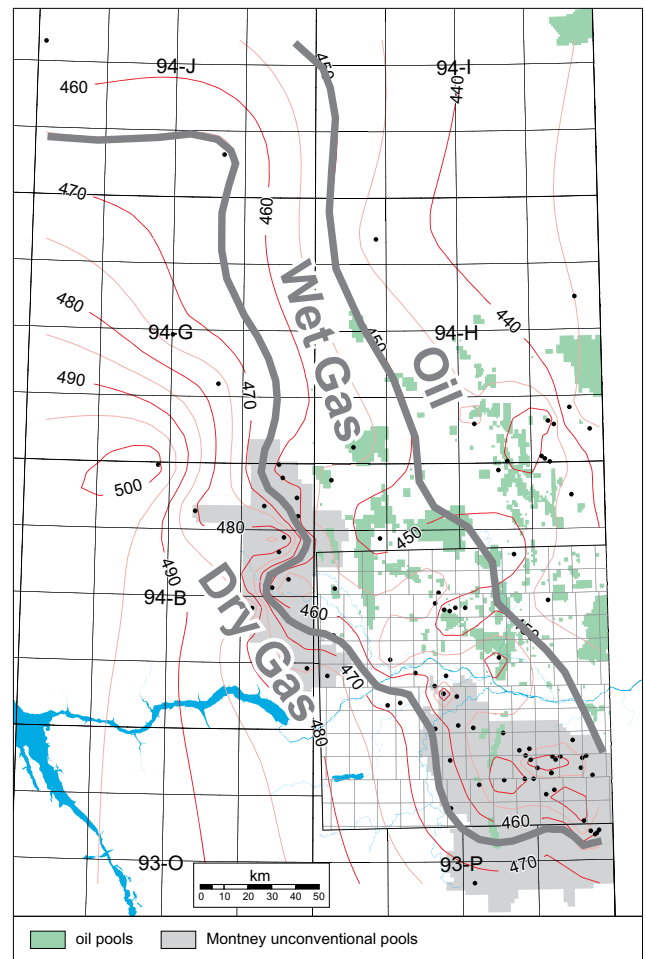


Figure 14. Zones of dry gas, wet gas and wet gas to oil within the Montney Formation derived from  $T_{max}$  data. Wet gas generation is bracketed between 450 and 465°C  $T_{max}$  values (Fig. 4), with peak wet gas generation along the 455°C line.

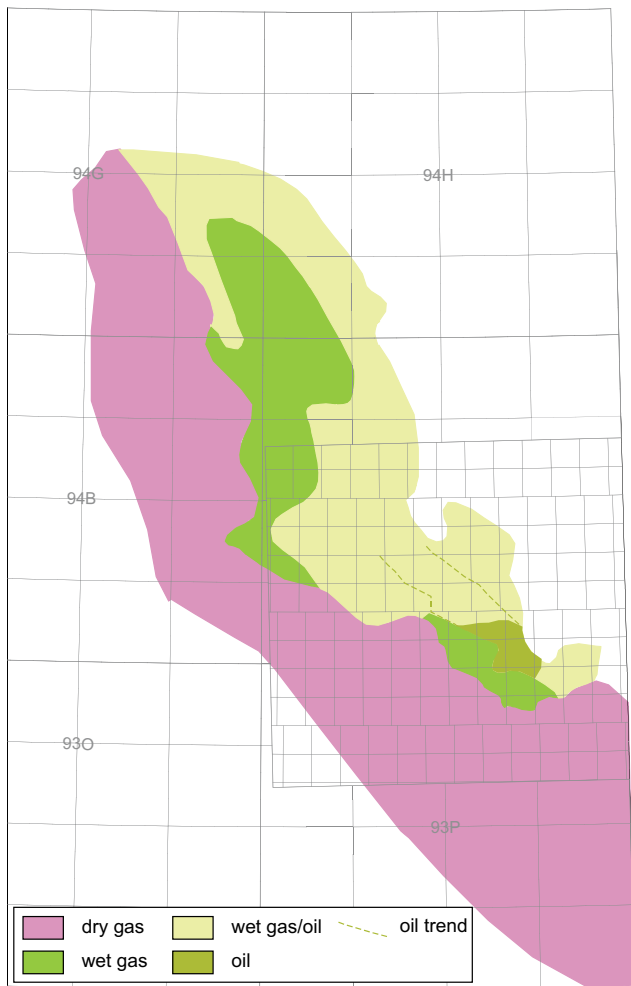


Figure 15. Zones of dry gas, wet gas, wet gas+oil and oil within the Montney Formation derived from sales gas data.

## REFERENCES

- Bordenave, M.L. (1993): Applied Petroleum Geochemistry; *Technip*, Paris, 531 pages.
- Dewing, K. and Sanei, H. (2009): Analysis of large thermal maturity datasets: examples from the Canadian Arctic Islands; *International Journal of Coal Geology*, Volume 77, pages 436–448.
- Espitalié, J., Deroo, G. and Marquis, F. (1985a): Rock-Eval pyrolysis and its applications (part two); *Institut Français du Pétrole*, Oil & Gas Science and Technology, Volume 40, pages 755–784.
- Espitalié, J., Deroo, G. and Marquis, F. (1985b): Rock-Eval pyrolysis and its applications (part one); *Institut Français du Pétrole*, Oil & Gas Science and Technology, Volume 40, pages 563–579.
- Espitalié, J., Deroo, G. and Marquis, F. (1986): Rock-Eval pyrolysis and its applications (part three); *Institut Français du Pétrole*, Oil & Gas Science and Technology, Volume 41, pages 73–89.
- Ferri, F., Hayes, M. and Goodman, E. (2013): Core and cuttings analysis, northeast British Columbia; *British Columbia Ministry of Natural Gas Development*, Petroleum Geology Open File, 2013-1.
- Fowler, M.G., Obermajer, M. and Snowdon, L.R. (2007a): Rock-Eval/TOC data for eleven NE British Columbia boreholes (map areas 94-I to 94-P); *Geological Survey of Canada*, Open File 5672.
- Fowler, M.G., Obermajer, M. and Snowdon, L.R. (2007b): Rock-Eval/TOC data for eight NE British Columbia boreholes (map areas 93-O to 94-H); *Geological Survey of Canada*, Open File 5673.
- Fowler, M.G. and Snowdon, L.R. (2001): Rock-Eval/TOC data for ten northern Alberta and British Columbia wells; *Geological Survey of Canada*, Open File 4124.
- Ibrahimbas, A. and Riediger, C.L. (2004): Hydrocarbon source rock potential as determined by Rock-Eval 6/TOC pyrolysis, northeast British Columbia and Northwest Alberta; in Summary of Activities 2004, *British Columbia Ministry of Energy, Mines and Natural Gas*, pages 8–18.
- Jacob, H. (1985): Disperse solid bitumen as an indicator for migration and maturity in prospecting for oil and gas; *Erdol Kohle*, Volume 38, pages 365–374.
- Jarvie, D.M. (1991): Total organic carbon (TOC) analysis; in Source migration processes and evaluation techniques; Merrill, R.K., Editor, *American Association of Petroleum Geologists*, Treatise of Petroleum Geology, pages 113–118.
- Langford, F.F. and Blanc-Valleron, M.-M. (1990): Interpreting Rock-Eval pyrolysis data using graphs of pyrolyzable hydrocarbons vs. total organic carbon; *American Association of Petroleum Geologists Bulletin*, Volume 74, pages 799–804.
- Lafargue, E., Marquis, F. and Pillot, D. (1998): Rock-Eval 6 applications in hydrocarbon exploration, production, and soil contamination studies; *Revue de L'institut Français du Pétrole*, Volume 53, pages 421–437.
- Peters, K.E. (1986): Guidelines for evaluating petroleum source rock using programmed pyrolysis; *American Association of Petroleum Geologists Bulletin*, Volume 70, pages 318–329.

- Riediger, C.L. (1990): Rock-Eval/TOC data from the Lower Jurassic “Nordegg Member”, and the Lower and Middle Triassic Doig and Montney formations, Western Canada Sedimentary Basin, Alberta and British Columbia; *Geological Survey of Canada*, Open File 2308.
- Snowdon, L.R. (2000): Rock-Eval/TOC data for three British Columbia wells; *Geological Survey of Canada*, Open File 3910.
- Teichmuller, M. and Durand, B. (1983): Fluorescence microscopical rank studies on liptinites and vitrinites in peat and coals, and comparison with results of the rock-eval pyrolysis; *International Journal of Coal Geology*, Volume 2, Issue 3, pages 197–230.
- Tissot, B. and Welte, D.N. (1984): Petroleum Formation and Occurrence, 2nd edition; *Springer Verlag*, Heidelberg, 699 pages.
- Walsh, W. and McPhail, S. (2007): Shale gas potential: core and cuttings analysis, northeast British Columbia; *British Columbia Ministry of Energy, Mines and Natural Gas*, Petroleum Geology Open File 2007-1.

